Acta Crystallographica Section F
Structural Biology and Crystallization Communications
ISSN 1744-3091

Crystallization and preliminary X-ray diffraction studies of a terminal oxygenase of carbazole 1,9a-dioxygenase from *Novosphingobium* sp. KA1

Takashi Umeda,[a]‡ Junichi Katsuki,[a]‡ Yuji Ashikawa,[a,b] Yusuke Usami,[a] Kengo Inoue,[a,c] Haruko Noguchi,[a,d] Zui Fujimoto,[e] Hisakazu Yamane[a] and Hideaki Nojiri[a,d]*

[a]Biotechnology Research Center, The University of Tokyo, 1-1-1 Yayoi, Bunkyo-ku, Tokyo 113-8657, Japan, [b]Molecular Signaling Research Team, Structural Physiology Research Group, RIKEN Harima Institute SPring-8 Center, 1-1-1 Kouto, Sayo, Hyogo 679-5148, Japan, [c]Interdisciplinary Research Organization, University of Miyazaki, 5200 Kihara, Kiyotake, Miyazaki 889-1692, Japan, [d]Professional Programme for Agricultural Bioinformatics, The University of Tokyo, 1-1-1 Yayoi, Bunkyo-ku, Tokyo 113-8657, Japan, and [e]Protein Research Unit, National Institute of Agrobiological Sciences, 2-1-2 Kannondai, Tsukuba, Ibaraki 305-8602, Japan

‡ These authors contributed equally to this paper.

Correspondence e-mail: anojiri@mail.ecc.u-tokyo.ac.jp

Received 12 July 2010
Accepted 30 August 2010

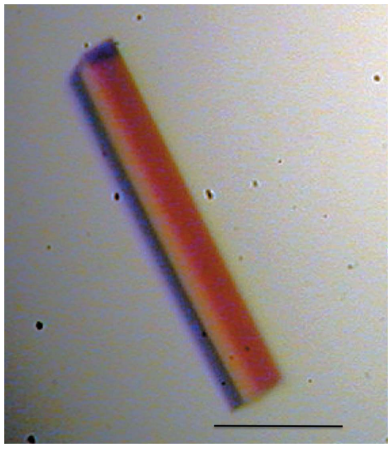

Carbazole 1,9a-dioxygenase (CARDO) is the initial dioxygenase in the carbazole-degradation pathway of *Novosphingobium* sp. KA1. The CARDO from KA1 consists of a terminal oxygenase (Oxy), a putidaredoxin-type ferredoxin and a ferredoxin reductase. The Oxy from *Novosphingobium* sp. KA1 was crystallized at 277 K using the hanging-drop vapour-diffusion method with ammonium sulfate as the precipitant. Diffraction data were collected to a resolution of 2.1 Å. The crystals belonged to the monoclinic space group $P2_1$. Self-rotation function analysis suggested that the asymmetric unit contained two Oxy trimers; the Matthews coefficient and solvent content were calculated to be 5.9 Å^3 Da^{-1} and 79.1%, respectively.

1. Introduction

Carbazole, a toxic and carcinogenic compound (Sverdrup *et al.*, 2002; Jha & Bharti, 2002), is a component of creosote, crude oil and shale oil (Mushrush *et al.*, 1999). In order to investigate the biodegradation of this N-heterocyclic aromatic compound in contaminated soil, many carbazole-degrading bacteria have been isolated. From analyses of the metabolism of carbazole by several bacteria, genes encoding carbazole-degradative enzymes, called the *car* gene cluster, have been found. Subsequent enzymatic investigation revealed the importance of carbazole 1,9a-dioxygenase (CARDO) as the initial catalyst in the carbazole-degradation pathway (Nojiri & Omori, 2007).

CARDO catalyzes regioselective and stereoselective dihydroxylation of the angular (C_{9a}) and adjacent (C_1) C atoms of carbazole. CARDO consists of a terminal oxygenase (Oxy; encoded by the *carAa* gene) and the electron-transfer components ferredoxin (Fd; encoded by the *carAc* or *fdx* gene) and ferredoxin reductase (Red; encoded by the *carAd* or *fdr* gene). The electron required for the oxidation of carbazole is transferred from NAD(P)H to Oxy (Fig. 1). *Novosphingobium* sp. KA1 possesses the carbazole-degradative plasmid pCAR3, which contains two *car* gene clusters involved in carbazole assimilation and several orphan genes for electron transfer (*carAaIAcI*, *carAaIIAcII*, *fdxI* and *fdrI*/*fdrII*; Urata *et al.*, 2006).

CARDO is a member of the Rieske nonhaem iron oxygenases (ROs) that are found in various species of bacteria. ROs have been divided into five subgroups (IA, IB, IIA, IIB and III) based on the number of constituents and the nature of their redox centres (Batie *et al.*, 1991). The CARDOs of KA1 are classified as class IIA ROs, while the well studied CARDOs from *Pseudomonas resinovorans* CA10, *Janthinobacterium* sp. J3 and *Nocardioides aromaticivorans* IC177 belong to classes III, III and IIB, respectively (Nojiri & Omori, 2007). In this paper, the Oxys from KA1, CA10, J3 and IC177 are abbreviated Oxy_{IIA}, Oxy_{III}, Oxy_{III} and Oxy_{IIB}, respectively. The same method of abbreviation is used for the Fds and Reds of each strain.

Several recent studies have described the structure of RO oxygenases such as naphthalene dioxygenase (Kauppi *et al.*, 1998), biphenyl dioxygenase (Furusawa *et al.*, 2004), 2-oxoquinoline 8-monooxygenase (Martins *et al.*, 2005) and dicamba monooxygenase (D'Ordine *et al.*, 2009; Dumitru *et al.*, 2009). Naphthalene dioxygenase and biphenyl dioxygenase exist as $\alpha_3\beta_3$ heterohexamers. CARDO, 2-oxoquinoline 8-monooxygenase and dicamba mono-

oxygenase form α_3 homotrimers and phthalate dioxygenase is thought to be an $\alpha_3\alpha_3$ homohexamer (Tarasev *et al.*, 2007).

To date, we have determined the crystal structures of several components of CARDO: Fd_{III} from *P. resinovorans* CA10 (Nam *et al.*, 2005), Oxy_{III} from *Janthinobacterium* sp. J3 (Nojiri *et al.*, 2005) and the Oxy_{III}–Fd_{III} electron-transfer complex (Ashikawa *et al.*, 2006) and Oxy_{IIB} and Fd_{IIB} from *N. aromaticivorans* (Inoue *et al.*, 2009). We have also successfully crystallized Fd_{IIA} and Red_{IIA} from *Novosphingobium* sp. KA1 (Umeda *et al.*, 2008, 2010) and Red_{III} from *Janthiobacterium* sp. J3 (Ashikawa *et al.*, 2007) and the structures of these proteins have been solved (Ashikawa *et al.*, in preparation; Umeda *et al.*, in preparation).

This report describes the crystallization and preliminary X-ray diffraction study of Oxy_{IIA} (encoded by *carAaII*; a trimer of 383 residues with a molecular mass of 129.3 kDa).

2. Materials and methods

2.1. Protein expression and purification

The DNA fragment containing the *carAaII* gene, corresponding to amino acids 1–383 of Oxy_{IIA} (NCBI accession No. YP_717942), was amplified from the total DNA of *Novosphingobium* sp. KA1 by PCR using the following oligonucleotide primers containing artificial *Nde*I and *Xho*I sites (shown in bold): 5′-AAAAAA**CATATG**CAGACGG-CAAGCGTCCCGGC-3′ and 5′-AAAAAA**CTCGAG**TCGGACG-TCCCTCGTCTGGA-3′. The PCR product was digested with *Nde*I and *Xho*I and then ligated into the corresponding sites of pET26b(+), which expresses full-length Oxy_{IIA} with an LEHHHHHH tag that replaces the termination codon. The integrity of the cloned constructs was confirmed by DNA sequencing and the plasmid was designated pEKA232. *Escherichia coli* BL21 (DE3) cells (Novagen, Wisconsin, USA; Merck, Darmstadt, Germany) transformed with pEKA232 were grown in 5 ml lysogeny medium (10 g l^{-1} tryptone peptone, 5 g l^{-1} yeast extract and 10 g l^{-1} NaCl; Sambrook & Russell, 2001) supplemented with 50 µg ml^{-1} kanamycin at 310 K. After overnight incubation, the whole culture was added to 1.5 l SB medium (24 g yeast extract, 12 g tryptone, 3.8 g KH_2PO_4, 12.5 g K_2HPO_4 and 5 ml glycerol per litre) and cultivation was carried out at 298 K and 120 rev min^{-1}. When the optical density at 600 nm reached 0.5, isopropyl D-β-1-thiogalactopyranoside was added to a final concentration of 0.5 m*M*. After 15 h incubation, the cells were harvested by centrifugation (5000*g*, 10 min), washed twice with TG buffer (20 m*M* Tris–HCl pH 7.5 and 10% glycerol) and resuspended in buffer *A* (TG buffer containing 0.5 *M* NaCl). Following cell lysis by sonication on ice, the lysate was clarified by centrifugation (25 000*g*, 60 min). All purification procedures were carried out at 277 K. The supernatant was applied onto a HiTrap Chelating HP column (GE Healthcare, Uppsala, Sweden) on an ÄKTA FPLC instrument (GE Healthcare). Oxy_{IIA} was eluted using a gradient of 10–200 m*M* imidazole in buffer *A*. The fraction containing Oxy_{IIA} was buffer-exchanged with GFC buffer (20 m*M* Tris–HCl pH 7.5, 0.2 *M* NaCl and 10% glycerol) and concentrated by ultrafiltration using a Centriprep YM-10 (Millipore, Massachusetts, USA). The concentrated solution was loaded onto a Superdex 200 prep-grade column (GE Healthcare) pre-equilibrated with GFC buffer. The eluate was buffer-exchanged with crystallization buffer (5 m*M* Tris–HCl pH 7.5) and concentrated as described above. The homogeneity of Oxy_{IIA} was confirmed by SDS–PAGE. Protein concentrations were estimated using a protein-assay kit (Bio-Rad) with BSA as the standard (Bradford, 1976).

Table 1
Crystal parameters and data-collection statistics.

Values in parentheses are for the highest resolution shell.

Beamline	NW12A
Wavelength (Å)	1.000
Detector	ADSC Quantum Q210
Crystal-to-detector distance (mm)	164
Rotation range per image (°)	0.5
Total rotation range (°)	270
Exposure time per image (s)	5
Resolution range (Å)	50.0–2.10
Space group	$P2_1$
Unit-cell parameters (Å, °)	a = 117.1, b = 159.0, c = 167.8, $\alpha = \gamma$ = 90.0, β = 94.5
Mosaicity (°)	0.26
Total No. of reflections	2038550
No. of unique reflections	355075 (35357)
Multiplicity	5.7 (5.7)
Average $I/\sigma(I)$	31.5 (3.5)
Completeness (%)	99.9 (100)
R_{merge}† (%)	7.4 (43.6)
Overall B factor from Wilson plot (Å^2)	12.0

† $R_{merge} = \sum_{hkl}\sum_i |I_i(hkl) - \langle I(hkl)\rangle| / \sum_{hkl}\sum_i I_i(hkl)$, where $I_i(hkl)$ is the ith observation of reflection hkl and $\langle I(hkl)\rangle$ is the weighted average intensity for all observations i of reflection hkl.

2.2. Crystallization

Crystallization experiments were performed at 278 K using the hanging-drop vapour-diffusion method; initial trials were carried out using Crystal Screen, Crystal Screen 2, Crystal Screen Cryo, Index

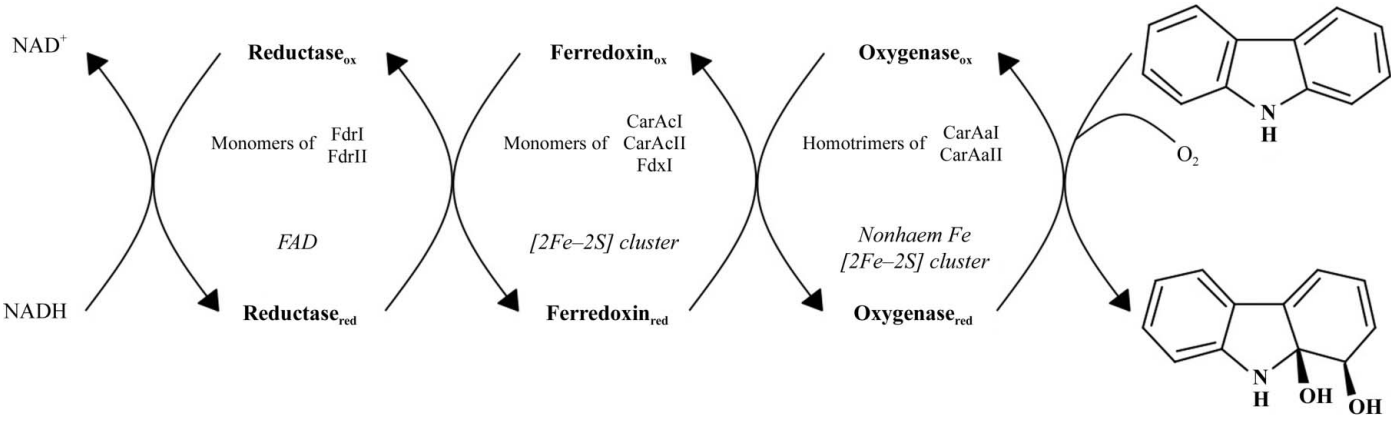

Figure 1
Components and functions of the class IIA CARDO system. The proposed electron-transfer and dioxygenation reactions are illustrated. The cofactors of each component are shown in italics. The subscripts 'ox' and 'red' indicate oxidized and reduced states of the CARDO components, respectively.

and Grid Screen Ammonium Sulfate (Hampton Research, California, USA). Hanging drops, each consisting of 3 µl reservoir solution and 3 µl 20 mg ml^{-1} protein solution, were equilibrated against 600 µl reservoir solution. Oxy_{IIA} crystals were obtained using Crystal Screen Cryo condition No. 4 (0.075 *M* Tris–HCl pH 8.5, 1.5 *M* ammonium sulfate and 25% glycerol) after 3–5 d incubation. After several rounds of optimization, a single crystal grew after 3 d at 278 K using a protein concentration of 20 mg ml^{-1} and a reservoir solution consisting of 25% glycerol, 1.5 *M* ammonium sulfate and 0.1 *M* Tris–HCl pH 8.5. Finally, the above-mentioned reservoir solution was mixed with 0.1 *M* calcium chloride as an additive reagent in a 4:1 ratio to set up hanging drops. The resulting solution and 20 mg ml^{-1} protein solution were mixed in equal amounts to obtain the crystals used for X-ray diffraction data collection.

2.3. X-ray diffraction data collection

The crystals were scooped into a nylon cryoloop and directly flash-cooled in a nitrogen stream at 100 K. Diffraction experiments were conducted on beamline NW12A at the Photon Factory, Tsukuba, Japan. The data were collected at a wavelength of 1.000 Å using a Quantum 210 CCD X-ray detector (ADSC, California, USA). A complete diffraction data set consisting of 540 images with an oscillation angle of 0.5° and 5 s exposure per image was collected to a resolution of 2.1 Å. Diffraction data were indexed, integrated and scaled using *HKL*-2000 (Otwinowski & Minor, 1997). Data-collection and processing statistics are listed in Table 1.

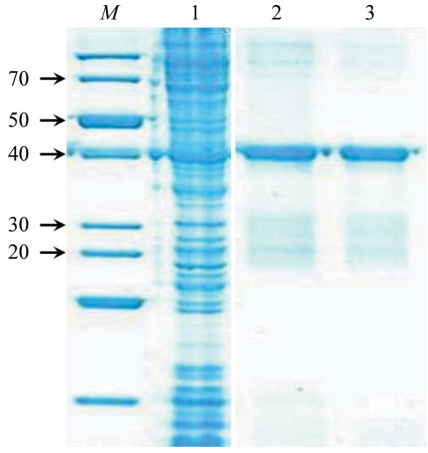

Figure 2
SDS–PAGE of Oxy_{IIA}. Samples were loaded onto a 12% polyacrylamide gel in the presence of SDS. Lane *M*, protein markers (kDa); lane 1, cell lysate; lane 2, pooled fraction containing Oxy_{IIA} after affinity chromatography; lane 3, fraction containing Oxy_{IIA} after gel-filtration chromatography.

Figure 3
An Oxy_{IIA} crystal. The scale bar indicates 0.3 mm.

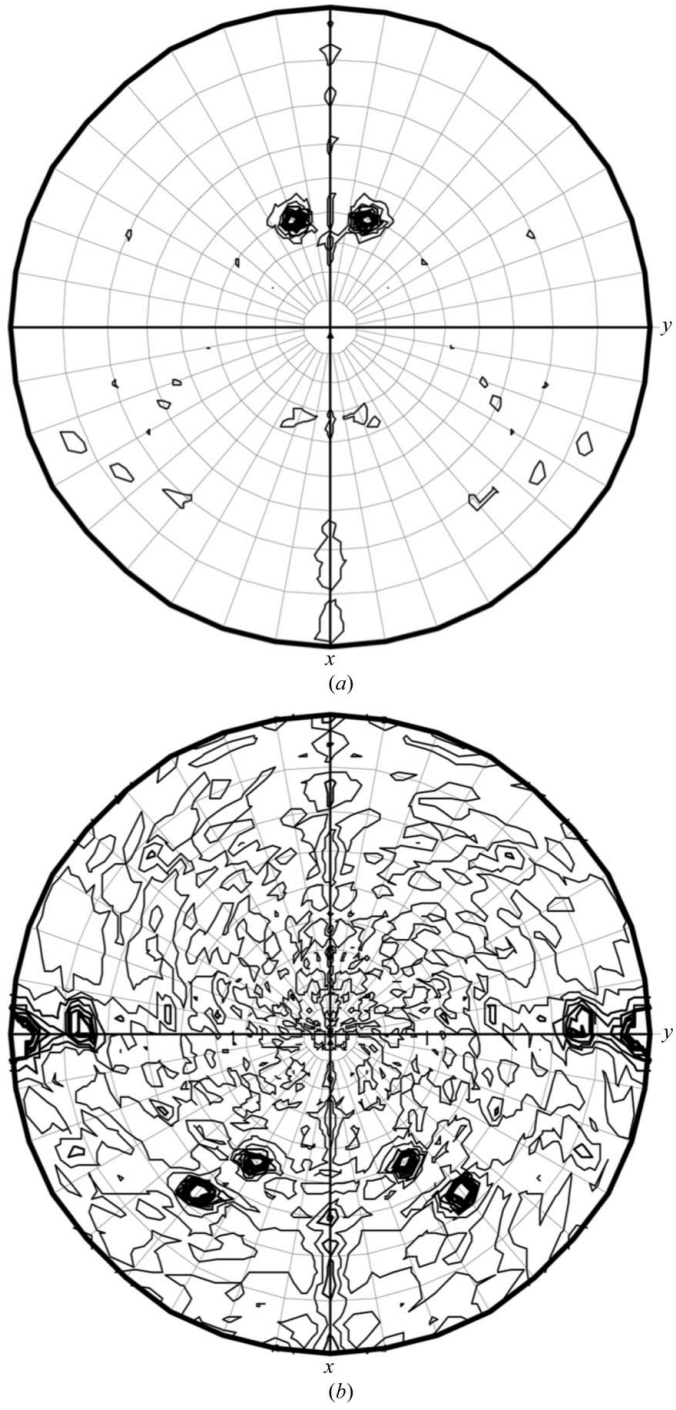

Figure 4
Self-rotation function map based on structure-factor amplitudes collected from a crystal of Oxy_{IIA}. The (*a*) $\kappa = 120°$ and (*b*) $\kappa = 180°$ sections are shown for a self-rotation function calculated with all data in the resolution range 10–3 Å with a radius of integration of 30 Å.

3. Results and discussion

The amount of Oxy_{IIA} harvested was approximately 5 mg per litre of SB culture. SDS–PAGE analysis estimated the purified Oxy_{IIA} to be >95% pure (Fig. 2). As with the other classes of Oxys, Oxy_{IIA} eluted as a trimer from gel-filtration chromatography (data not shown).

The crystals of Oxy_{IIA} grew to dimensions of 0.2 × 0.2 × 1.0 mm after 3 d and belonged to space group $P2_1$, with unit-cell parameters $a = 117.1$, $b = 159.0$, $c = 167.8$ Å, $\alpha = \gamma = 90$, $\beta = 94.5^\circ$ (Fig. 3). Based on Matthews coefficient calculations (Matthews, 1968), between four (58.2% solvent content) and seven trimers (26.8% solvent content) could be accommodated in the asymmetric unit, with an acceptable packing density V_M in the range 1.68–2.94 Å^3 Da^{-1}. A self-rotation function was calculated from the scaled data from 10 to 3.0 Å resolution using *MOLREP* (Collaborative Computational Project, Number 4, 1994; Vagin & Teplyakov, 2010) and the sections with $\kappa = 180^\circ$ and 120° showed significant peaks (Fig. 4). The peaks in the $\kappa = 120^\circ$ section were assigned to a head-to-tail homotrimeric Oxy_{IIA} quaternary structure and the peaks in the $\kappa = 180^\circ$ section were considered to originate from the presence of twofold noncrystallographic symmetry. These data indicated that there were two Oxy_{IIA} trimers in the asymmetric unit, corresponding to an unusual packing density V_M of 5.9 Å^3 Da^{-1} (79.1% solvent content) for the Oxy_{IIA} crystal. The quaternary structure of Oxy_{IIA} was assumed to be doughnut-shaped, with a hole at the centre of the Oxy_{IIA} structure. It was supposed that water molecules can enter into this hole. This is likely to be a factor in the high solvent content. A full description of the structure determination and interpretation of the structure–function relationship will be published elsewhere.

This work was supported by a Grant-in-Aid for Scientific Research (20248010 to HN) from the Ministry of Education, Culture, Sports, Science and Technology of Japan and by the Institute for Bioinformatics Research Development, Japan Science Technology Agency (BIRD-JST). The use of synchrotron radiation was approved by the Photon Factory Advisory Committee and KEK (High-Energy Accelerator Research Organization), Tsukuba, Japan (proposals 2004G137, 2006G171, 2007G135 and 2008G681). TU was supported by Research Fellowships from the Japan Society for the Promotion of Science for Young Scientists.

References

Ashikawa, Y., Fujimoto, Z., Noguchi, H., Habe, H., Omori, T., Yamane, H. & Nojiri, H. (2006). *Structure*, **14**, 1779–1789.
Ashikawa, Y., Uchimura, H., Fujimoto, Z., Inoue, K., Noguchi, H., Yamane, H. & Nojiri, H. (2007). *Acta Cryst.* F**63**, 499–502.
Batie, C. J., Ballou, D. P. & Correll, C. C. (1991). *Chemistry and Biochemistry of Flavoenzymes*, Vol. 3, edited by F. Muller, pp. 543–556. Boca Raton: CRC Press.
Bradford, M. M. (1976). *Anal. Chem.* **72**, 248–254.
Collaborative Computational Project, Number 4 (1994). *Acta Cryst.* D**50**, 760–763.
D'Ordine, R. L., Rydel, T. J., Storek, M. J., Sturman, E. J., Moshiri, F., Bartlett, R. K., Brown, G. R., Eilers, R. J., Dart, C., Qi, Y., Flasinski, S. & Franklin, S. J. (2009). *J. Mol. Biol.* **392**, 481–497.
Dumitru, R., Jiang, W. Z., Weeks, D. P. & Wilson, M. A. (2009). *J. Mol. Biol.* **392**, 498–510.
Furusawa, Y., Nagarajan, V., Tanokura, M., Masai, E., Fukuda, M. & Senda, T. (2004). *J. Mol. Biol.* **342**, 1041–1052.
Inoue, K., Ashikawa, Y., Umeda, T., Abo, M., Katsuki, J., Usami, Y., Noguchi, H., Fujimoto, Z., Terada, T., Yamane, H. & Nojiri, H. (2009). *J. Mol. Biol.* **392**, 436–451.
Jha, A. M. & Bharti, M. K. (2002). *Mutat. Res.* **500**, 97–101.
Kauppi, B., Lee, K., Carredano, E., Parales, R. E., Gibson, D. T., Eklund, H. & Ramaswamy, S. (1998). *Structure*, **6**, 571–586.
Martins, B. M., Svetlitchnaia, T. & Dobbek, H. (2005). *Structure*, **13**, 817–824.
Matthews, B. W. (1968). *J. Mol. Biol.* **33**, 491–497.
Mushrush, G. W., Beal, E. J., Hardy, D. R. & Hughes, J. R. (1999). *Fuel Proc. Technol.* **61**, 197–210.
Nam, J.-W., Noguchi, H., Fujimoto, Z., Mizuno, H., Ashikawa, Y., Abo, M., Fushinobu, S., Kobashi, N., Wakagi, T., Iwata, K., Yoshida, T., Habe, H., Yamane, H., Omori, T. & Nojiri, H. (2005). *Proteins*, **58**, 779–789.
Nojiri, H., Ashikawa, Y., Noguchi, H., Nam, J.-W., Urata, M., Fujimoto, Z., Uchimura, H., Terada, T., Nakamura, S., Shimizu, K., Yoshida, T., Habe, H. & Omori, T. (2005). *J. Mol. Biol.* **351**, 355–370.
Nojiri, H. & Omori, T. (2007). *Pseudomonas*, Vol. 5, edited by J. L. Ramos & A. Filloux, pp. 107–145. New York: Springer.
Otwinowski, Z. & Minor, W. (1997). *Methods Enzymol.* **276**, 307–326.
Sambrook, J. & Russell, D. W. (2001). *Molecular Cloning: A Laboratory Manual*, 3rd ed. New York: Cold Spring Harbor Laboratory Press.
Sverdrup, L. E., Jensen, J., Kelley, A. E., Krogh, P. H. & Stenersen, J. (2002). *Environ. Toxicol. Chem.* **21**, 109−114.
Tarasev, M., Kaddis, C. S., Yin, S., Loo, J. A., Burgner, J. & Ballou, D. P. (2007). *Arch. Biochem. Biophys.* **466**, 31−39.
Umeda, T., Katsuki, J., Ashikawa, Y., Usami, Y., Inoue, K., Noguchi, H., Fujimoto, Z., Yamane, H. & Nojiri, H. (2010). *Acta Cryst.* F**66**, 712–714.
Umeda, T., Katsuki, J., Usami, Y., Inoue, K., Noguchi, H., Fujimoto, Z., Ashikawa, Y., Yamane, H. & Nojiri, H. (2008). *Acta Cryst.* F**64**, 632–635.
Urata, M., Uchimura, H., Noguchi, H., Sakaguchi, T., Takemura, T., Eto, K., Habe, H., Omori, T., Yamane, H. & Nojiri, H. (2006). *Appl. Environ. Microbiol.* **72**, 3198–3205.
Vagin, A. & Teplyakov, A. (2010). *Acta Cryst.* D**66**, 22–25.